




## Black Sea hydroclimate and coupled hydrology was strongly controlled by high-latitude glacial climate dynamics

Antje Wegwerth <sup>1✉</sup>, Birgit Plessen <sup>2</sup>, Ilka C. Kleinhanns<sup>3</sup> & Helge W. Arz <sup>1✉</sup>

The Black Sea experienced pronounced millennial-scale changes in temperature and rainfall during the last glacial coinciding with Dansgaard-Oeschger cycles. However, little is known regarding the amount and sources of freshwater reaching this inland basin. Here, we present detailed ostracod  $\delta^{18}\text{O}$  data from the glacial Black Sea showing subdued Dansgaard-Oeschger cyclicity and four prominent longer-term saw-tooth shaped Bond-like cycles. We propose that the  $\delta^{18}\text{O}_{\text{ostracods}}$  signature primarily reflects changes in the atmospheric circulation in response to the waxing and waning Eurasian Ice Sheet. The millennial-scale ice sheet variations likely resulted not only in latitudinal migrations of atmospheric frontal systems but also in shifts of dominant moisture sources for the Black Sea. Heavier isotopic precipitation arrived from the North Atlantic-Mediterranean realm during the warmer interstadials and lighter isotopic precipitation from the Eurasian continental interior during the colder stadials. The subdued Dansgaard-Oeschger variability likely reflects an integrated precipitation signal additionally affected by the long mixing times of the large Black Sea volume up to 1,500 years as suggested from hydrologic-isotope-balance modelling.

<sup>1</sup>Leibniz Institute for Baltic Sea Research Warnemünde (IOW), Marine Geology, Rostock, Germany. <sup>2</sup>Helmholtz Centre Potsdam, GFZ German Research Centre for Geosciences, Section Climate Dynamics and Landscape Evolution, Potsdam, Germany. <sup>3</sup>Isotope Geochemistry, Department of Earth Sciences, University of Tübingen, Tübingen, Germany. ✉email: [antje.wegwerth@io-warnemuende.de](mailto:antje.wegwerth@io-warnemuende.de); [helge.arz@io-warnemuende.de](mailto:helge.arz@io-warnemuende.de)

To understand hemisphere-wide climate variability during glacials, profound knowledge of former oceanic and atmospheric coupling in a zonal and meridional perspective is essential requiring well-preserved palaeo-archives that are widely distributed over the oceans and continents. While especially records along the North Atlantic recording last glacial orbital- and millennial-scale climate variability are available, high-resolution continental records from the last glacial are still sparse. However, just the deeper continental palaeoclimate records may allow retracing high to mid-latitude teleconnection patterns of the atmospheric circulation system tightly coupled to the size of the Eurasian Ice Sheet during glacials. The former glacial isolated Black Sea, bridging the North Atlantic–Eurasian corridor, is one of such inland candidates. It could help to extend our view of high- to midlatitude atmospheric coupling during glacial climate variability.

During the relatively mild period within the last glacial between 57 and 29 ka BP, the Marine Isotope Stage 3 (MIS 3<sup>1</sup>), temperatures fluctuated on a millennial time scale during the so-called Dansgaard–Oeschger cycles (DO cycles) with abrupt warming into interstadials and gradual cooling into stadials across the North Atlantic–Mediterranean corridor<sup>2–7</sup>. During MIS 3, the largely enclosed, lacustrine Black Sea experienced pronounced DO climate and environmental variability as well, which were tightly linked to changes in the North Atlantic Meridional Overturning Circulation (AMOC) and temperature variations in Greenland<sup>7–9</sup>. Temperature amplitudes between stadials and interstadials in the Black Sea were as high as 4 °C<sup>7</sup>. During the warmer interstadials, the amount of rainfall and riverine freshwater supply into the basin increased<sup>8,9</sup>. The increased freshwater contribution resulted in increased lake level and lower salinity, whereas higher nutrient supply and warmer conditions favoured primary productivity. In Northern Anatolia, temperate forest expanded and wind strength was reduced<sup>8,9</sup>. During the colder stadials, the hydroclimate gradually changed from humid to arid conditions, which resulted in increased evaporation, a lowered lake level, and higher salinity. Along with reduced riverine supply of nutrients, primary productivity decreased. During stadial winters, temperatures were much lower than during interstadial winters resulting in ice formation at the southern coast of the Black Sea ‘Lake’<sup>7–10</sup>. On land, the vegetation in Northern Anatolia became dominant in xerophytic steppe<sup>8</sup>. In a long-term perspective, similar changes in temperature and especially in rainfall amounts on an orbital timescale are superimposed to the DO-cycles with much more humid conditions during the first half of MIS 3<sup>8,9</sup>. During this time window it is supposed that the enhanced supply of freshwater by rainfall and rivers caused a rising lake level of the Black Sea that probably resulted into an overflow into the Marmara Sea until ca. 42 ka BP<sup>9,11–13</sup>.

Previous studies have contributed to the knowledge about the changes in temperature and rainfall amount and the resulting environmental implications for the Black Sea ‘Lake’ and Northern Anatolia during MIS 3<sup>7–10</sup>. In addition to the Black Sea sediment record, the  $\delta^{18}\text{O}$  records of speleothems from Northern Anatolia document these climate cycles exceptionally well and are suggested to reflect changes in the  $\delta^{18}\text{O}$  composition of the Black Sea surface water<sup>14</sup>. However, there is no clear explanation for the underlying processes and mechanisms of these apparent changes in the  $\delta^{18}\text{O}$  composition of the Black Sea surface waters during the intermediate climate state of Marine Isotope Stage 3 (57–29 ka BP). Therefore, it has to be unravelled how these changes relate to the variability of temperature, the amount and sources of rainfall and riverine supply as well as to the hydrological activity in the Black Sea itself. With a deeper knowledge of the coupling between hydroclimate variability and hydrological activity, it may help understanding continental high- to mid-latitude teleconnection patterns of the atmospheric circulation

during glacials. Here, we present a new continuous high-resolution  $\delta^{18}\text{O}$  record obtained from benthic ostracod carbonate shells from a well-dated SE Black Sea sediment core in order to investigate the hydrological dynamics in the former Black Sea upper water column and their relation to migrating air mass trajectories subjected to hydroclimate reorganisations. In combination with a well-dated  $\delta^{18}\text{O}$  record from speleothems of the Northern Anatolian Sofular Cave that has been suggested to mainly reflect the  $\delta^{18}\text{O}$  composition of the former Black Sea surface water during the period of interest<sup>14,15</sup>, we will propose potential atmospheric-hydroclimatic processes explaining the similar and diverging trends in both records. We further will elaborate on why the  $\delta^{18}\text{O}$  record has a significant orbital timescale component and how this is related to the Eurasian Ice Sheet (EIS) dynamics and changes in atmospheric circulation patterns over Eurasia. A simple hydrologic-isotope-balance model will show that the  $\delta^{18}\text{O}_{\text{ostracods}}$  pattern reflects an integrated central European precipitation signal with its imprint strongly affected by hydrological activity and mixing times of the large water volume of the Black Sea. A new  $^{87}\text{Sr}/^{86}\text{Sr}_{\text{ostracods}}$  record obtained from the same sediment core, will serve for estimating changes in the dominant source of riverine supply that might be partially associated with meltwater release from the EIS in turn potentially affecting the  $\delta^{18}\text{O}$  composition of the Black Sea.

Today, the Black Sea is a semi-enclosed, brackish basin and represents the largest anoxic water body on Earth<sup>16,17</sup>. It receives freshwater by rivers and rainfall and saltwater by the inflow of water from the Mediterranean and Marmara Seas through the Dardanelles and Bosphorus straits<sup>17</sup>. Due to the higher input of freshwater by precipitation (P) and riverine runoff (R) compared to the loss of water by evaporation (E), the modern Black Sea has a positive water balance ( $P + R > E$ )<sup>17</sup>.

Controlled by the northern hemispheric atmospheric circulation over Europe, the climate in the Black Sea region is mainly controlled by the Polar Front Jet, the mid- to high latitude westerlies, the Subtropical Jet, and the Siberian and the mid-latitude subtropical high pressure systems<sup>18,19</sup> (Fig. 1). The dynamics and intensity of Mediterranean cyclones arriving in the Black Sea are affected by the East African and Indian monsoons in combination with the Siberian high-pressure system and relate to the positions of the Polar Front and Subtropical Jet<sup>18,19</sup>. With dry summers and wet winters, the Black Sea climate is generally under Mediterranean influence and its interannual variability is strongly linked to the North Atlantic Oscillation<sup>20–25</sup>. Mediterranean atmospheric moisture mainly originates from the North Atlantic, but evaporation of Mediterranean waters also strongly controls the isotopic composition of rainfall in the Black Sea drainage basin<sup>26</sup>.

Northeastern Anatolia and the eastern Black Sea are the most summer rain-laden Black Sea regions due to orographic precipitation in the Pontic and Caucasian Mountains<sup>27–29</sup>, whereas the Black Sea itself forms an additional moisture source for rainfall<sup>14,15,24</sup>.

On an over-regional scale, the  $\delta^{18}\text{O}$  composition of rainfall across Eurasia decreases progressively from the mid-latitudes to northern latitudes and generally eastwards to the continental interior (Fig. 1) due to the Rayleigh condensation<sup>30–32</sup>. The  $\delta^{18}\text{O}$  composition of rainfall in the Black Sea region ranges today from  $-4\text{‰}$  to  $-8\text{‰}$ <sup>33</sup>, whereas other studies reported even values of around  $-9\text{‰}$ <sup>34</sup>. Additionally to the rainout effect with depletion towards northeast and the continent, the altitude of the NE Anatolian Mountains also affects the rainfall isotopic composition leading to values of about  $-10\text{‰}$ <sup>26</sup>. Today, in the Black Sea the  $\delta^{18}\text{O}$  composition of the surface water ranges between  $-2.44\text{‰}$  and  $-2.84\text{‰}$ <sup>15,33,35,36</sup>, whereas the deeper water is slightly heavier and reveals a composition between  $-1.65\text{‰}$  and  $-1.8\text{‰}$ <sup>33,35,36</sup>. However, it has to be noted that during strong precipitation periods, the oxygen isotopic composition of the

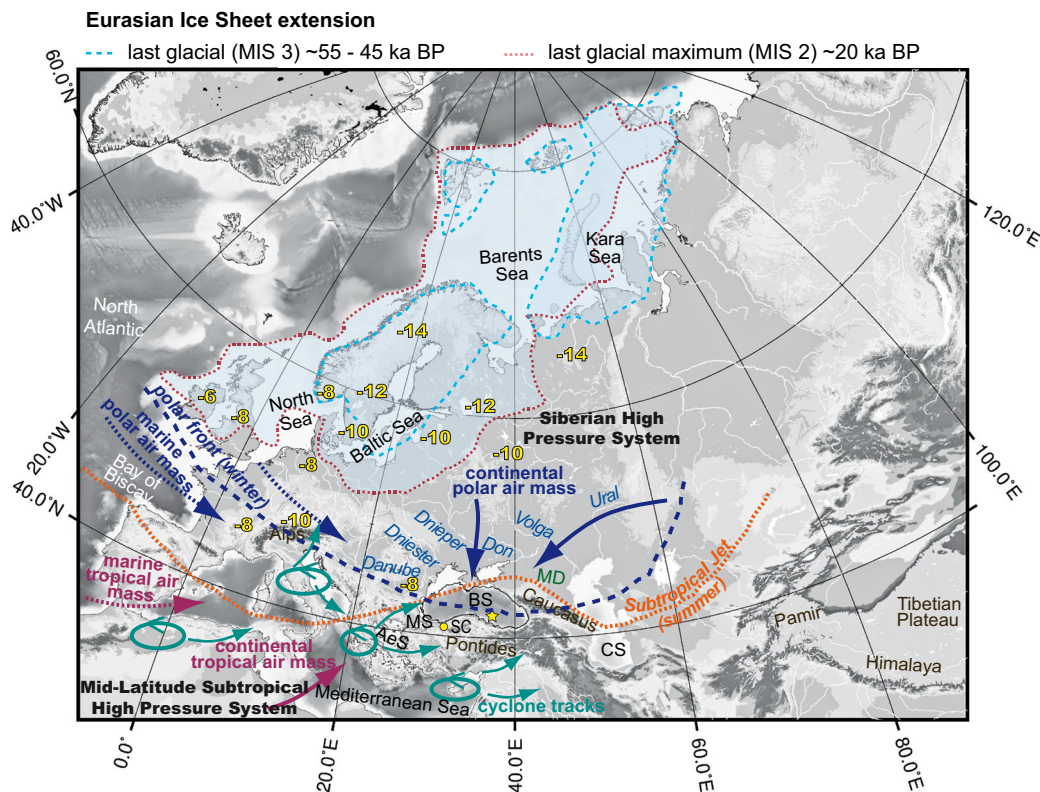


**Fig. 1 Map showing Eurasia.** Location of the coring site of M72/5 25GC-1 in the Black Sea (yellow star), and the maximum extent of the Eurasian Ice Sheet during the Weichselian (blue shading; MIS 2 and 3; modified from Larsen et al.<sup>73</sup>). Idealised scheme of the modern atmospheric circulation patterns with broad position of the polar front during January and the Subtropical Jet during July influencing regional climate in the Black Sea region (modified after Wigley and Farmer<sup>18</sup>; Akçar and Schlüchter<sup>19</sup>). Yellow numbers show values for the  $\delta^{18}\text{O}$  composition of modern rainfall<sup>53</sup>. AeS = Aegean Sea, BS = Black Sea, CS = Caspian Sea, MD = Manych Depression, MS = Marmara Sea, SC = Sofular Cave (Map modified after Wegwerth et al.<sup>39</sup>).

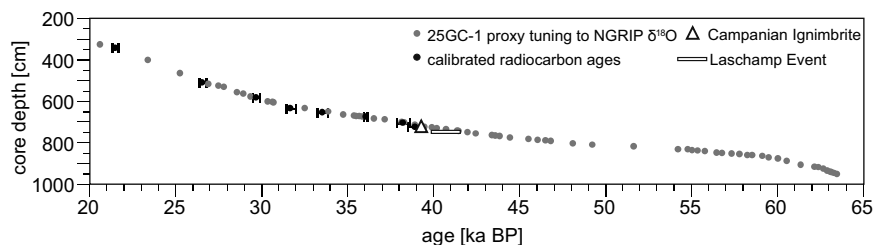


**Fig. 2 Core chronology.** Age-depth model of sediment core M72/5 25GC-1 between 20 and 65 ka BP, error bars define age uncertainties (slightly modified from Nowaczyk et al. and Wegwerth et al.<sup>7,9,10</sup>).

surface water can decrease to  $-7.1\text{‰}$ <sup>33</sup>, demonstrating the pronounced sensitivity of the Black Sea to variations in freshwater input. With 50–70% of the total riverine input, the Danube river is the main freshwater source from all rivers draining into the Black Sea today<sup>17,37</sup>. Near the river mouth, the Danube reveals a  $\delta^{18}\text{O}$  composition of  $-10.5\text{‰}$ <sup>36</sup>. While the freshwater contributed by rivers and rainfall is isotopically highly depleted, the high-salinity Mediterranean water entering the Black Sea has a  $\delta^{18}\text{O}$  composition of about  $+1.8\text{‰}$ <sup>33</sup>.

**Results**

The presented data derive from the well-dated<sup>10</sup> gravity core M72/5 25GC-1 recovered at the Archangelsky Ridge in the SE Black Sea ( $42^{\circ}06.20'\text{N}$ ,  $36^{\circ}37.40'\text{E}$ ) in a water depth of 418 m (Figs. 1 and 2).

**$\delta^{18}\text{O}_{\text{ostracods}}$ .** The Black Sea  $\delta^{18}\text{O}_{\text{ostracods}}$  record covering the last glacial from MIS 4 to MIS 2 (64–20 ka BP; Fig. 3b) shows values ranging between  $-2.7\text{‰}$  and  $-6.1\text{‰}$  (Supplementary Data 1). During the first half of MIS 3, the values of  $\delta^{18}\text{O}_{\text{ostracods}}$  are less depleted (or show maximum values) reaching a level similar to the last two glacial–interglacial transitions<sup>38,39</sup>. Else than several other parameters already presented from the same sediment core for that period<sup>7–10</sup>, the  $\delta^{18}\text{O}_{\text{ostracods}}$  apparently do not reveal only the typical millennial-scale Dansgaard–Oeschger pattern. Instead, the  $\delta^{18}\text{O}_{\text{ostracods}}$  signature clearly shows four cycles with sharply increasing (lasting 1–3 kyrs) and gradually decreasing (lasting 3–8 kyrs) values with minima occurring close to the onset of North Atlantic Heinrich stadials. From MIS 4 towards MIS 2,  $\delta^{18}\text{O}_{\text{ostracods}}$  values are getting lighter during each cycle finally culminating in minimum values around the last glacial maximum (LGM) at 23 ka BP.

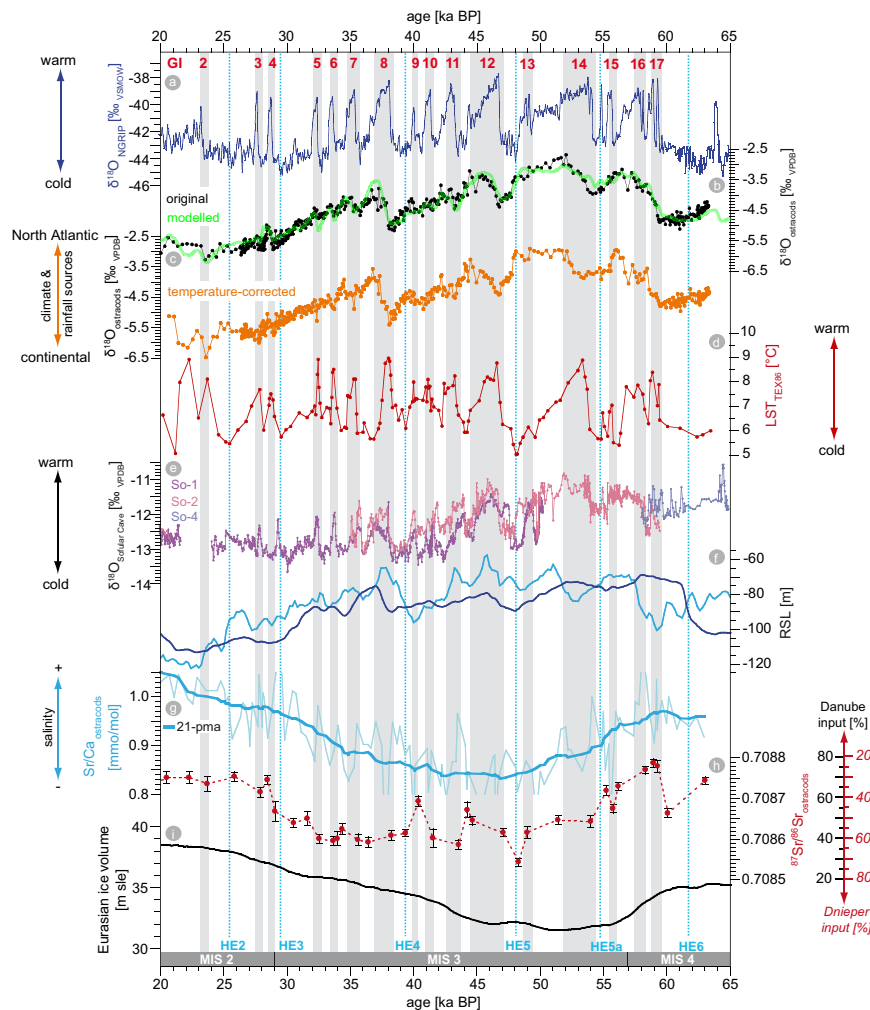


**Fig. 3** Climate and environmental conditions in the Black Sea during the last glacial. **a**  $\delta^{18}\text{O}_{\text{NGRIP}}$  62–65 (Greenland) **b**  $\delta^{18}\text{O}_{\text{ostracods}}$  (original and modelled (Supplementary Information), this study); **c**  $\text{TEX}_{86}$ -temperature corrected  $\delta^{18}\text{O}_{\text{ostracods}}$  (this study); **d**  $\text{TEX}_{86}$ -based lake surface temperature<sup>7</sup> (LST); **e**  $\delta^{18}\text{O}_{\text{Sofular Cave}}$  (stalagmites So-1, So-2, and So-4<sup>14,15</sup>); **f** relative sea level (light blue: Arz et al.<sup>66</sup>; dark blue: Grant et al.<sup>67</sup>); **g**  $\text{Sr}/\text{Ca}_{\text{ostracods}}$  indicating changes in salinity<sup>9</sup> (raw data and simple 21-point moving average); **h**  $^{87}\text{Sr}/^{86}\text{Sr}_{\text{ostracods}}$  indicating changes in river sources (this study), error bars define standard errors, estimation of relative changes in the contributions between Danube (0.7089)<sup>50</sup> and Dnieper (0.7084)<sup>50</sup>; **i** Eurasian ice volume<sup>45</sup> (m sea level equivalent). The red numbers and grey bars denote the Greenland Interstadials (GI) during Dansgaard-Oeschger cycles and the blue numbers denote Heinrich event (HE) equivalent periods.

**$^{87}\text{Sr}/^{86}\text{Sr}_{\text{ostracods}}$ .** The Sr-isotope record of the ostracods shows a relatively low variability ranging between 0.708546 and 0.708789 (average 0.708670;  $n = 35$ ) with minimum values occurring during mid-MIS 3 and maximum values during MIS 4 and MIS 2 (Fig. 3h; Supplementary Data 1). Apart from some outliers during the middle part of MIS 3 between 40 and 45 ka BP, the  $^{87}\text{Sr}/^{86}\text{Sr}_{\text{ostracods}}$  pattern bears resemblance to the long-term pattern of the  $\text{Sr}/\text{Ca}_{\text{ostracods}}$  record, with its minimum level interpreted to reflect a freshening phase during MIS 3<sup>9</sup> (Fig. 3g).

## Discussion

**Potential factors changing the Black Sea  $\delta^{18}\text{O}_{\text{ostracods}}$  composition during the last glacial.** The high-resolution  $\delta^{18}\text{O}_{\text{ostracods}}$  record presented here on a centennial timescale reveals at first glance a subdued nature of DO variability suggesting that it neither reflects simply temperature nor rainfall amount since both abruptly changed during last glacial stadial-interstadial cycles in the Black Sea region<sup>7–9</sup>. The variations in the  $\delta^{18}\text{O}_{\text{ostracods}}$  record represent a combined response to changes in the  $\delta^{18}\text{O}$  composition of the water and in the ambient

temperature during the growth of the ostracod shells. The  $\delta^{18}\text{O}$  composition of the glacial lacustrine Black Sea water column, in turn, was affected by changes in a) evaporation of the lake surface and b) the amount, sources, and  $\delta^{18}\text{O}$  composition of freshwater input from direct precipitation at the lake surface and indirectly via rivers arriving from the Black Sea drainage basins. The latter isotopic signature comes from a mixture of precipitation and potential meltwater from adjacent glaciers and ice sheets feeding the rivers<sup>38,40,41</sup>. In case of a connection to the Black Sea via the Manych depression, Caspian water could have additionally contributed to an altered (lighter)  $\delta^{18}\text{O}$  composition because rainfall as well as river Volga ( $\delta^{18}\text{O}$ :  $-12.5\text{‰}$ ) contributing by 80% of total riverine discharge into the Caspian Sea are isotopically very light<sup>15,42</sup>. Otherwise, a connection to the Mediterranean Sea would have led to increased  $\delta^{18}\text{O}$  values<sup>38</sup>.

In addition to the above mentioned potential external factors, internal features such as long residence times of the water could modulate the  $\delta^{18}\text{O}$  composition of the ostracods. Thus, longer mixing times of the water column associated with reduced freshwater input may cause an overprint of the pattern of the  $\delta^{18}\text{O}_{\text{ostracods}}$  resulting in an orbital-scale pattern by the loss of an

original millennial-scale climate component, especially for mixing times that are on the scale of individual DO-cycles.

When affected only by temperature, the range of about 3.4‰ in the  $\delta^{18}\text{O}_{\text{ostracods}}$  would suggest temperature amplitudes of about 13.6 °C during the investigated period<sup>43,44</sup>. However, temperature changes between stadials and interstadials reached only up to 4 °C during the period 64–20 ka BP as revealed by reconstructions of TEX<sub>86</sub>-based annual lake surface temperatures<sup>7</sup> (Fig. 3d). Similarly, estimations of temperature changes in the intermediate water depth of ~400 m by Mg/Ca<sub>ostracods</sub> imply temperature amplitudes of 2–4 °C during the DO-cycles<sup>7</sup>. This circumstance and because the record a) lacks clear millennial-scale DO variability and b) shows generally higher values during warmer periods although the opposite pattern (negative correlation) would be expected, the temperature impact on the  $\delta^{18}\text{O}_{\text{ostracods}}$  was most likely very low<sup>43,44</sup>.

By considering a relation of 0.25‰ decrease in  $\delta^{18}\text{O}$  per rise of 1 °C in temperature<sup>43,44</sup>, we corrected the  $\delta^{18}\text{O}_{\text{ostracods}}$  values by removing this temperature effect using the TEX<sub>86</sub>-based lake surface temperatures from the same sediment core<sup>7</sup> to unfold a potential DO variability not coupled to temperature. Although this lake surface temperature correction relative to the conditions at the ostracod's habitat depth at 418 m represents an over-correction, the temperature-corrected  $\delta^{18}\text{O}_{\text{ostracods}}$  values are very much the same as the non-corrected values (Fig. 3c) confirming another superordinate environmental factor for the  $\delta^{18}\text{O}_{\text{ostracods}}$  composition of the Black Sea 'Lake'.

Similar to an enhanced temperature, increased input of freshwater by rivers including meltwater discharge would result in lowered  $\delta^{18}\text{O}$  values. Previous studies have demonstrated a pronounced variability in the amount of riverine input on orbital- and millennial timescales from different proxies from the same sediment core presented in this study<sup>8,9</sup>. Since riverine discharge includes both direct rainfall and meltwater, we try to unravel the impact of these different freshwater sources on the  $\delta^{18}\text{O}_{\text{ostracods}}$  record in this chapter. Irrespective of the freshwater source, an increase must have lowered the  $\delta^{18}\text{O}$  composition of the water in the Black Sea basin. On a millennial timescale, rainfall was much higher during the warmer interstadials as indicated by an increased arboreal pollen abundance reflecting the expansion of moisture-dependent temperate forest vegetation<sup>8</sup>. The related riverine discharge likely lowered the surface water salinity as mirrored by decreasing Sr/Ca<sub>ostracods</sub> and increased freshwater dinoflagellate assemblages during interstadials<sup>8,9</sup> (Fig. 3g). Furthermore, the amount of leaf wax derived odd-numbered long-chain *n*-alkanes along with the sedimentary ln(K/Ti) ratio, both reflecting relative changes between riverine and aeolian input, support the observation of an amplified riverine discharge during interstadials<sup>9</sup>.

In addition to the DO-patterns, the long-term patterns of the aforementioned proxies suggest a pronounced orbital-scale component with increased freshwater supply during the first and warmer half of MIS 3 strongly resembling the pattern of the coevally reduced Eurasian Ice Sheet volume<sup>45</sup> (Fig. 3i). Therefore, in addition to rainfall, increased meltwater discharge originating from the Eurasian Ice Sheet could have affected the hydrology and salinity of the former Black Sea 'Lake'. Similar as during other meltwater pulses during the last two glacial terminations and the deeper penultimate glacial, the Dnieper could have played an increasing role in freshwater discharge relative to the Danube<sup>39,46,47</sup>. A reliable tool for estimating changes in river sources for the glacial Black Sea is the Sr-isotopic composition of ostracods<sup>39,47,48</sup>, because it depends on the catchment geology in the respective drainage regions<sup>48,49</sup>. Our new <sup>87</sup>Sr/<sup>86</sup>Sr<sub>ostracods</sub> record (Fig. 3h) shows generally less radiogenic values when compared to the last two glacial-interglacial

terminations (T I<sup>48</sup>: 0.709102; T II<sup>47</sup>: 0.709452) and the penultimate glacial (MIS 6<sup>39</sup>; max. 0.709405) and lowest values are reached during MIS 3 (0.7085460) with a slightly elevated glacial background during the colder periods (MIS 4 and 2: 0.708789). These values indicate an increased contribution of Dnieper and Don relative to Danube<sup>50</sup> including meltwater from the partly disintegrating Eurasian Ice during the earlier part of MIS 3<sup>45</sup>. When disregarding runoff from the remaining smaller rivers, our estimations imply that the contribution by Dnieper relative to Danube could have increased up to 71% during MIS 3, whereas during MIS 4 and 2 the relative contribution by Danube would have amounted up to 78% (Fig. 3h). A certain contribution from Caspian waters (<sup>87</sup>Sr/<sup>86</sup>Sr: 0.70821–0.7085) via spill out along the Manych depression (Fig. 1) is possible as well<sup>50–52</sup>. Although not explicitly suggested from the Sofular Cave speleothem  $\delta^{18}\text{O}$  record, the dinoflagellate assemblages from the Black Sea sediment core would be in line with a potential Caspian connection<sup>8,15</sup>.

Despite the clear evidence for early MIS 3 meltwater contribution, the amount released by the medium sized MIS 3 ice sheet<sup>45</sup> was obviously insufficient for decreasing the  $\delta^{18}\text{O}$  composition of the Black Sea water column as it was the case for the meltwater pulses of the last two glacial terminations and the deeper penultimate glacial<sup>38,39,47</sup>. Comparable trends in the  $\delta^{18}\text{O}_{\text{ostracods}}$ , <sup>87</sup>Sr/<sup>86</sup>Sr<sub>ostracods</sub> and EIS volume records (Fig. 3b, h, i), however, suggest changes in the atmospheric circulation over the North Atlantic and Eurasia as a potential trigger of the observed patterns. Alike the Black Sea ostracod record, the  $\delta^{18}\text{O}$  values from the speleothems of Sofular Cave in north-western Anatolia are also heavier during the more humid interstadials than during the stadial periods<sup>14,15</sup> (Fig. 3e). While the speleothem data are suggested to be closely linked to the surface water conditions of the former Black Sea 'Lake'<sup>14</sup>, it is conceivable that the  $\delta^{18}\text{O}_{\text{Sofular Cave}}$  was affected not only by the Black Sea as moisture source<sup>14</sup>, but incorporated a variable portion of heavier atmospheric moisture signal originating in the (eastern) Mediterranean Sea and the North Atlantic.

Since a retreated Eurasian Ice Sheet was most likely associated with a northward migration of the atmospheric polar front, precipitation patterns and moisture sources may have changed as well. The northward migration of the frontal systems over Eurasia possibly caused a progressively stronger influence of the North Atlantic/Mediterranean moisture sources to the precipitation in the Black Sea region and could explain a shift towards a heavier  $\delta^{18}\text{O}$  signature. Arppe and Karhu<sup>53</sup> pointed out that present precipitation patterns over Europe with a westerly moisture source and a progressive isotopic depletion in the heavier isotopes of air masses towards northeast existed also during MIS 3. Based on  $\delta^{18}\text{O}$  analyses of mammoth tooth enamel and palaeogroundwaters across Europe, the authors reconstructed the oxygen isotopic composition of rainfall for the period 52–24 ka BP, showing ca. 2‰ lighter values relative to present<sup>53</sup>. Although there are no reconstructions of  $\delta^{18}\text{O}$ -precipitation patterns over Eurasia available for more discrete intervals or even on a millennial timescale, the general reconstruction for the MIS 3 implies lighter  $\delta^{18}\text{O}$  values in SE Europe when the Eurasian Ice Sheet was present (MIS 3) than it was absent (today)<sup>53</sup>. This supports the idea of the MIS 3 Eurasian Ice Sheet dynamics as an important forcing factor in modulating the Eurasian atmospheric circulation pattern and moisture sources of the Black Sea region.

According to reconstructions by Bintanja and van de Wal<sup>45</sup>, the Eurasian Ice Sheet began to expand again since ca. 40 ka BP (Fig. 3i). Accordingly, a repeated southward migration of the atmospheric polar front is indicated from 40 ka BP by increasing wind intensity and drier conditions in SE Europe as reconstructed from grain-size distribution of loess-palaeosol sequences in the Lower Danube Basin<sup>54</sup>. The authors argue for an increasing role

of the Siberian/Eurasian high-pressure system in modulating the continentality towards the peak glacial phase (Fig. 1). Such a gradual change likely reduced the North Atlantic/Mediterranean sourced precipitation in the Black Sea region causing a strong negative trend in the  $\delta^{18}\text{O}_{\text{ostracods}}$  record due to increased contribution of rainfall sourced in the Eurasian continental interior. On the millennial scale, the stronger imprint of Heinrich stadials compared to the regular stadials in the  $\delta^{18}\text{O}_{\text{ostracods}}$  record would then similarly point to a major reorganisation of the atmospheric circulation with a stronger continentality and much lighter  $\delta^{18}\text{O}_{\text{ostracods}}$ . This goes in hand with the expected direct effect from the condensation temperature of moisture sources above the cave and more generally the Black Sea drainage basin with lighter (heavier)  $\delta^{18}\text{O}$  at low (high) stadial (interstadial) temperatures.

**Changes in the Black Sea ‘Lake’ hydrology during the last glacial.** On the millennial scale the  $\delta^{18}\text{O}_{\text{ostracods}}$  record is not following simply the DO pattern, but appears to be subdued and slightly delayed regarding the peak interstadials. This may be caused by variable mixing times of the relatively large Black Sea ‘Lake’ water body in response to the hydrological balance of the basin. Similar to our MIS 3 record,  $\delta^{18}\text{O}_{\text{ostracods}}$  records from the western Black Sea of the last glacial maximum and Termination I show rather smoothly increasing values and lack a clear shift during the Bölling-Alleröd warming and the cold Younger Dryas stadial<sup>38,55,56</sup>.

The present Black Sea water residence time is in an order of 1000 years<sup>57</sup> but it might have varied significantly during the last glacial period. It can be assumed that the mixing time in a basin of that size and geometry could have lasted as long as or even longer than an average DO cycle resulting in a significant modification of an original freshwater input signal. The mixing time during the late MIS 3/MIS 2 increased potentially to several millennia in response to the generally aridification trend towards the LGM with a negative hydrological balance in the basin. Higher evaporation and a decreasing Black Sea ‘Lake’ level is indicated e.g., by increased salinities as reconstructed by  $\text{Sr}/\text{Ca}_{\text{ostracods}}$ , sequence-stratigraphic evidence of an LGM lake level low stand in the Danube fan area<sup>58</sup>, and significantly higher reservoir ages of up to 1450 years towards the LGM<sup>10,59,60</sup>.

Following the approach by Bahr et al.<sup>38</sup> performing a simplified hydrologic-isotope-balance model (HIBAL<sup>61</sup>) for the Black Sea since the LGM, we simulated the  $\delta^{18}\text{O}$  composition of the Black Sea for the period 64–20 ka BP by considering potential changes in the amount of precipitation, runoff, and evaporation, which consequently involves changes in the mixing time of the Black Sea water. As a high-latitude rainfall source we used the  $\delta^{18}\text{O}_{\text{NGRIP}}$ <sup>62–65</sup> record (Supplementary Methods, Supplementary Table S1, Supplementary Fig. S1). Supplementary Table S1 shows under which specific but simplified boundary conditions during four time slices our simulated  $\delta^{18}\text{O}$  record best mimic the measured  $\delta^{18}\text{O}_{\text{ostracods}}$  record (Fig. 3b, c; Supplementary Fig. S1).

Considering a reservoir age of 1450 years for the LGM around 23 ka BP<sup>10</sup> lying in our fourth time slice 20–28 ka BP of our HIBAL estimations (Supplementary Table S1), mixing times for the other three time slices can be roughly estimated from the hydrologic input volumes and are ~1500 years for 65–60 ka BP, ~700 years for 60–45 ka BP, and ~1000 years for 45–28 ka BP. These simulations support not only a high-latitude rainfall source, but also long and varying mixing times of the Black Sea water explaining the subdued nature of DO-variability in the intermediate water depth of the glacial, lacustrine Black Sea. For instance, during the earlier part of MIS 3 predominantly more humid conditions and a certain contribution by meltwater<sup>8,9</sup>

suggest a generally more enhanced hydrological activity. These conditions caused a rising lake level that probably culminated into an overflow into the Marmara Sea<sup>9,11–13</sup> associated with reduced mixing times and lower reservoir ages<sup>10,60</sup> being half as high as during the ending MIS 4 and towards the LGM.

Interestingly, the Bond-cycle like pattern in the  $\delta^{18}\text{O}_{\text{ostracods}}$  with a subdued DO-variability is remarkable similar to the pattern of global sea-level changes<sup>66,67</sup> (Fig. 3 b, c, f). It was proposed that gradual sea-level rises were related to interstadial warming and resulted mainly from melting of northern hemisphere ice sheets<sup>66</sup>. Obviously, the oxygen isotopic composition in the isolated Black Sea ‘Lake’ was not directly affected by such changes, but centennial scale changes in the dynamics of the Eurasian Ice Sheet and modified atmospheric teleconnections between the North Atlantic and Eurasia<sup>7</sup> might have had an additional imprint on the  $\delta^{18}\text{O}_{\text{ostracods}}$ .

The new high-resolution  $\delta^{18}\text{O}_{\text{ostracods}}$  record covering the last glacial from 64 to 20 ka BP along with the hydrologic-isotope-balance estimations demonstrates that the hydroclimate regime in the Black Sea region was strongly coupled to the northern hemisphere climate variations. During periods of a retreated Eurasian Ice Sheet, the  $\delta^{18}\text{O}_{\text{ostracods}}$  generally increase, which is likely related to the northward migrations of atmospheric frontal systems and a reduced continentality with an increasing influence from North Atlantic/Mediterranean moisture sources for the Black Sea region. Although the decreased  $^{87}\text{Sr}/^{86}\text{Sr}_{\text{ostracods}}$  values during the milder MIS 3 point to an increased meltwater contribution from the Dnieper, Don, and possibly Volga rivers, the effect is not evident in the  $\delta^{18}\text{O}_{\text{ostracods}}$  record. The subdued nature of the Dansgaard–Oeschger pattern recorded in the  $\delta^{18}\text{O}_{\text{ostracods}}$  we attribute to the long mixing times of the former Black Sea ‘Lake’ reacting sensitive to hydrological changes in the basin. We suggest generally shorter mixing times in an order of ~700 years in an overflowing and fresher Black Sea in the first warmer and more humid part of MIS 3 and increasing mixing times up to ~1500 years during the later part of MIS 3 and during MIS 2 and late MIS 4 with generally more arid conditions and a lowered lake level.

## Methods

**Sediment core and chronology.** This study bases on the gravity core 25GC-1 recovered during RV Meteor cruise M72/5 in the SE Black Sea in 2007 (Fig. 1; Archangelsky Ridge, 42°06.20’N, 36°37.40’E, 418 m water depth). The sediment core consists mainly of detrital mud intercalated by carbonate-rich intervals. The core chronology<sup>10</sup> (Fig. 2) bases on AMS radiocarbon dating, the Campanian ignimbrite tephra (Y5; 39.28 ± 0.11 ka<sup>68</sup>), the Laschamp geomagnetic excursion (40.70 ± 0.95 ka BP<sup>69</sup>), and proxy-tuning to the  $\delta^{18}\text{O}$  record from the North Greenland Ice core Project on the GICC05 timescale<sup>62–65</sup> (NGRIP). A study on cryotephra horizons from the same core largely confirmed the NGRIP-tuned stratigraphy<sup>70</sup>. The sequence of interest in the present study covering the last glacial from the late MIS 4 to the MIS 2 (64–20 ka BP) derives from core depth 307–952 cm.

**Ostracod isotope geochemistry.** For the analyses of the  $\delta^{18}\text{O}$  and  $^{87}\text{Sr}/^{86}\text{Sr}$  isotope signatures of the ostracods, well-preserved valves of adult specimens of *Candona* spp. were hand-picked from the wet-sieved and dried sediment fraction >150  $\mu\text{m}$ .

For the oxygen isotopic composition of the ostracods, the carbonate valves from 447 samples in total were cleaned with a thin brush and deionised water under a binocular microscope. Then, the pre-cleaned ostracods (20–80  $\mu\text{g}$ ) were measured with a Finnigan MAT 253 isotope ratio mass spectrometer coupled with an automated KIEL IV carbonate preparation device (103%  $\text{H}_3\text{PO}_4$  at 70 °C) at the GFZ Potsdam, Germany. Oxygen isotope values are given in delta notation relative to Vienna Pee Dee Belemnite. Repeated measurements of the international reference material NBS 19 and a laboratory internal standard (C1) assured an analytical precision better than ±0.07‰ for  $\delta^{18}\text{O}_{\text{ostracods}}$ .

For the analyses of the strontium isotopic composition, 35 samples evenly distributed along the core with each 10–15 ostracod valves were cleaned with a few drops of  $\text{H}_2\text{O}_2$  (5%), methanol, and deionised water<sup>48,71,72</sup>. After dissolution of the valves in 300  $\mu\text{L}$  2 vol%  $\text{HNO}_3$ , the samples were dried on a hot plate at 80 °C.

Strontium was separated from the sample matrix by using the  $\text{HNO}_3\text{-H}_2\text{O}$  technique in microcolumns filled with Eichrom<sup>®</sup> Sr-spec resin. Isotope analyses were performed with samples re-dissolved in 0.3 N  $\text{HNO}_3$  and all isotopic beams measured simultaneously in static mode on a MC-ICP-MS (Neptune Plus, Thermo) at the University of Tübingen, Germany. Instrumental mass bias was corrected using exponential law and an  $^{88}\text{Sr}/^{86}\text{Sr}$  ratio of 8.375209. External reproducibility for NBS SRM 987 was  $0.710253 \pm 0.000015$  (2 SD,  $n = 16$ ) for the  $^{87}\text{Sr}/^{86}\text{Sr}$  ratio and total procedural blank was  $<95.8$  pg Sr.

### Data availability

The data used in the present study are compiled in the Supplementary Data 1 and are freely available online at the data repository Zenodo (<https://doi.org/10.5281/zenodo.4545579>).

Received: 20 August 2020; Accepted: 18 February 2021;

Published online: 19 March 2021

### References

- Lisiecki, L. E. & Raymo, M. E. A Pliocene-Pleistocene stack of 57 globally distributed benthic  $\delta^{18}\text{O}$  records. *Paleoceanography* **20**, PA1003 (2005).
- Dansgaard, W. et al. Evidence for general instability of past climate from a 250-kyr ice-core record. *Nature* **364**, 218–220 (1993).
- Ganopolski, A. & Rahmstorf, S. Rapid changes of glacial climate simulated in a coupled climate model. *Nature* **409**, 153–158 (2001).
- Martrat, B. et al. Abrupt temperature changes in the western Mediterranean over the past 250,000 years. *Science* **306**, 1762–1765 (2004).
- Martrat, B. et al. Four climate cycles of recurring deep and surface water destabilizations on the Iberian margin. *Science* **317**, 502–507 (2007).
- Kindler, P. et al. Temperature reconstruction from 10 to 120 kyr b2k from the NGRIP ice core. *Clim. Past* **10**, 887–902 (2014).
- Wegwerth, A. et al. Black Sea temperature response to glacial millennial-scale climate variability. *Geophys. Res. Lett.* **42**, 8147–8154 (2015).
- Shumilovskikh, L. S. et al. Orbital- and millennial-scale environmental changes between 64 and 20 ka BP recorded in Black Sea sediments. *Clim. Past* **10**, 939–954 (2014).
- Wegwerth, A. et al. Northern hemisphere climate control on the environmental dynamics in the glacial Black Sea “Lake”. *Quat. Sci. Rev.* **135**, 41–53 (2016).
- Nowaczyk, N. R., Arz, H. W., Frank, U., Kind, J. & Plessen, B. Dynamics of the Laschamp geomagnetic excursion from Black Sea sediments. *Earth Planet. Sci. Lett.* **351–352**, 54–69 (2012).
- Çağatay, M. N. et al. Late Pleistocene-Holocene evolution of the northern shelf of the Sea of Marmara. *Mar. Geol.* **265**, 87–100 (2009).
- Aloisi, G. et al. Freshening of the Marmara Sea prior to its postglacial reconnection to the Mediterranean Sea. *Earth Planet. Sci. Lett.* **413**, 176–185 (2015).
- Çağatay, M. N. et al. The tephra record from the Sea of Marmara for the last ca. 70 ka and its palaeoceanographic implications. *Mar. Geol.* **361**, 96–110 (2015).
- Fleitmann, D. et al. Timing and climatic impact of Greenland interstadials recorded in stalagmites from northern Turkey. *Geophys. Res. Lett.* **36**, L19707 (2009).
- Badertscher, S. et al. Pleistocene water intrusions from the Mediterranean and Caspian seas into the Black Sea. *Nat. Geosci.* **4**, 236–239 (2011).
- Demailon, G. J. & Moore, G. T. Anoxic environments and oil source bed genesis. *Org. Geochem.* **2**, 9–31 (1980).
- Özsoy, E. & Ünlüata, Ü. Oceanography of the Black Sea: a review of some recent results. *Earth-Sci. Rev.* **42**, 231–272 (1997).
- Wigley, T. M. L. & Farmer, G. Climate of the Eastern Mediterranean and near east in *palaeoclimates, palaeoenvironments and human communities in the Eastern Mediterranean region of later prehistory* (Eds. J. L. Bintliff and W. van Zeist), pp. 3–39 B.A.R. International Series 133(i) (1982).
- Akçar, N. & Schlüchter, C. Paleoglaciations in Anatolia: a schematic review and first results in. *Eiszeitalter Gegenwart* **55**, 102–121 (2005).
- Cullen, H. M. & deMenocal, P. B. North Atlantic influence on Tigris–Euphrates streamflow. *Int. J. Climatol.* **20**, 853–863 (2000).
- Lamy, F., Arz, H. W., Bond, G. C., Bahr, A. & Pätzold, J. Multicentennial-scale hydrological changes in the Black Sea and northern Red Sea during the Holocene and the Arctic/North Atlantic Oscillation. *Paleoceanography* **21**, PA1008 (2006).
- Oguz, T., Dippner, J. W. & Kaymaz, Z. Climatic regulation of the Black Sea hydro-meteorological and ecological properties at interannual-to-decadal time scales. *J. Mar. Syst.* **60**, 235–254 (2006).
- Kwiecien, O. et al. North Atlantic control on precipitation pattern in the eastern Mediterranean/Black Sea region during the last glacial. *Quat. Res.* **71**, 375–384 (2009).
- Göktürk, O. M. et al. Climate on the southern Black Sea coast during the Holocene: implications from the Sofular Cave record. *Quat. Sci. Rev.* **30**, 2433–2445 (2011).
- Capet, A., Barth, A., Beckers, J.-M. & Marilaure, G. Interannual variability of Black Sea’s hydrodynamics and connection to atmospheric patterns. *Deep Sea Res. Part II: Top. Stud. Oceanogr.* **77–80**, 128–142 (2012).
- Roberts, N. et al. Stable isotope records of Late Quaternary climate and hydrology from Mediterranean lakes: the ISOMED synthesis. *Quat. Sci. Rev.* **27**, 2426–2441 (2008).
- Staneva, J. V. & Stanev, E. V. Oceanic response to atmospheric forcing derived from different climatic data sets. Intercomparison study for the Black Sea. *Oceanol. Acta* **21**, 393–417 (1998).
- Türkeş, M., Koç, T. & Sarıç, F. Spatiotemporal variability of precipitation total series over Turkey. *Int. J. Climatol.* **29**, 1056–1074 (2009).
- Deniz, A., Toros, H. & Incecik, S. Spatial variations of climate indices in Turkey. *Int. J. Climatol.* **31**, 394–403 (2011).
- Dansgaard, W. Stable isotopes in precipitation. *Tellus* **16**, 436–468 (1964).
- Bowen, G. J. & Wilkinson, B. Spatial distribution of  $\delta^{18}\text{O}$  in meteoric precipitation. *Geology* **30**, 315–318 (2002).
- Bowen, G. J. & Revenaugh, J. Interpolating the isotopic composition of modern meteoric precipitation. *Water Resour. Res.* **39**, <https://doi.org/10.1029/2003WR002086> (2003).
- Swart, P. K. The oxygen and hydrogen isotopic composition of the Black Sea. *Deep Sea Res. Part A. Oceanogr. Res. Pap.* **38**, S761–S772 (1991).
- Rozanski, K., Araguas-Araguas, L. & Gonfiantini, R. Isotopic patterns in modern global precipitation in *Climate change in continental isotopic records: American Geophysical Union Geophysical Monograph* **78**, pp. 1–36, <https://doi.org/10.1029/GM078p0001> (1993).
- Rank, D., Özsoy, E. & Salihoglu, İ. Oxygen-18, deuterium and tritium in the Black Sea and the Sea of Marmara. *J. Environ. Radioact.* **43**, 231–245 (1999).
- Özsoy, E., Rank, D. & Salihoglu, İ. Pycnocline and deep mixing in the black sea: stable isotope and transient tracer measurements. *Estuar. Coast. Shelf* **54**, 621–629 (2002).
- Nezlin, N. P. Seasonal and interannual variability of remotely sensed chlorophyll. In *The Black Sea environment*. Springer Berlin Heidelberg, pp. 333–350, <https://doi.org/10.1007/978-5-063> (2008).
- Bahr, A., Arz, H. W., Lamy, F. & Wefer, G. Late glacial to Holocene paleoenvironmental evolution of the Black Sea, reconstructed with stable oxygen isotope records obtained on ostracod shells. *Earth Planet. Sci. Lett.* **241**, 863–875 (2006).
- Wegwerth, A. et al. Major hydrological shifts in the Black Sea “Lake” in response to ice sheet collapses during MIS 6 (130–184 ka BP). *Quat. Sci. Rev.* **219**, 126–144 (2019).
- von Grafenstein, U., Erlenkeuser, H. & Trimborn, P. Oxygen and carbon isotopes in modern fresh-water ostracod valves: assessing vital offsets and autecological effects of interest for palaeoclimate studies. *Palaeogeogr. Palaeoclimatol. Palaeoecol.* **148**, 133–152 (1999).
- van Hardenbroek, M. et al. The stable isotope composition of organic and inorganic fossils in lake sediment records: current understanding, challenges, and future directions. *Quat. Sci. Rev.* **196**, 154–176 (2018).
- Sidorchuk, A. Y., Panin, A. V. & Borisova, O. K. Morphology of river channels and surface runoff in the Volga River basin (East European Plain) during the Late Glacial period. *Geomorphology* **113**, 137–157 (2009).
- McCrea, J. M. On the isotopic chemistry of carbonates and a paleotemperature scale. *J. Chem. Phys.* **18**, 849–857 (1950).
- Epstein, S., Buchsbaum, R., Lowenstam, H. A. & Urey, H. C. Revised carbonate-water isotopic temperature scale. *GSA Bull.* **64**, 1315–1326 (1953).
- Bintanja, R. & van de Wal, R. S. W. North American ice-sheet dynamics and the onset of 100,000-year glacial cycles. *Nature* **454**, 869–872 (2008).
- Soulet, G. et al. Abrupt drainage cycles of the Fennoscandian ice Sheet. *Proc. Nat. Acad. Sci. U.S.A.* **110**, 6682–6687 (2013).
- Wegwerth, A. et al. Meltwater events and the Mediterranean reconnection at the Saalian–Eemian transition in the Black Sea. *Earth Planet. Sci. Lett.* **404**, 124–135 (2014).
- Major, C. O. et al. The co-evolution of Black Sea level and composition through the last deglaciation and its paleoclimatic significance. *Quat. Sci. Rev.* **25**, 2031–2047 (2006).
- Reinhardt, E. G., Blenkinsop, J. & Patterson, R. T. Assessment of a Sr isotope vital effect ( $^{87}\text{Sr}/^{86}\text{Sr}$ ) in marine taxa from Lee Stocking Island, Bahamas. *Geo-Mar. Lett.* **18**, 241–246 (1998).
- Palmer, M. R. & Edmond, J. M. The strontium isotope budget of the modern ocean. *Earth Planet. Sci. Lett.* **92**, [https://doi.org/10.1016/0012-821X\(89\)90017-4](https://doi.org/10.1016/0012-821X(89)90017-4) (1989).
- Clauer, N., Chaudhuri, S., Toulkeridis, T. & Blanc, G. Fluctuations of Caspian Sea level: Beyond climatic variations? *Geology* **28**, 1015–1018 [https://doi.org/10.1130/0091-7613\(2000\)28<1015:FOCSLB>2.0.CO;2](https://doi.org/10.1130/0091-7613(2000)28<1015:FOCSLB>2.0.CO;2) (2000).

52. Page, A., Vance, D., Fowler, M. & Nisbet, E. Modern Sr isotopic mass balance and quaternary variation in the Caspian Sea. *EGS—AGU—EUG Joint Assembly*, Abstracts from the meeting held in Nice, France, 6–11 April 2003, abstract #3242 (2003).
53. Arrpe, L. & Karhu, J. A. Oxygen isotope values of precipitation and the thermal climate in Europe during the middle to late Weichselian ice age. *Quat. Sci. Rev.* **29**, 1263–1275 (2010).
54. Obrecht, I. et al. Shift of large-scale atmospheric systems over Europe during late MIS 3 and implications for Modern Human dispersal. *Sci. Rep.* **7**, 5848 (2017).
55. Kwiciczen, O. Paleo-environmental changes in the Black Sea region during the last 26,000 years: a multi-proxy study of lacustrine sediments from the western Black Sea. PhD-thesis, University of Potsdam, 98 p (2008).
56. Shumilovskikh, L. S. et al. Vegetation and environmental dynamics in the southern Black Sea region since 18 kyr BP derived from the marine core 22-GC3. *Palaeogeogr. Palaeoclimatol. Palaeoecol.* **337–338**, 177–193 (2012).
57. Östlund, H. G., Expedition “Odysseus 65”: radiocarbon age of Black Sea deep water. in *The Black Sea—geology, chemistry, and biology*. American Association of Petroleum Geologists Memoir 20, pp. 127–132, <https://doi.org/10.1306/M20377C40> (1974).
58. Constantinescu, A. M. et al. Evolution of the Danube deep-sea fan since the last glacial maximum: new insights into Black Sea water-level fluctuations. *Mar. Geol.* **367**, 50–68 (2015).
59. Kwiciczen, O. et al. Estimated reservoir ages of the black sea since the last glacial. *Radiocarbon* **50**, 99–118 (2008).
60. Soulet, G. et al. Black Sea “Lake” reservoir age evolution since the Last Glacial—hydrologic and climatic implications. *Earth Planet. Sci. Lett.* **308**, 245–258 (2011).
61. Benson, L. & Paillet, F. HIBAL: a hydrologic-isotopic-balance model for application to paleolake systems. *Quat. Sci. Rev.* **21**, 1521–1539 (2002).
62. Svensson, A. et al. The Greenland Ice Core Chronology 2005, 15–42ka. Part 2: comparison to other records. *Quat. Sci. Rev.* **25**, 3258–3267 (2006).
63. Svensson, A. et al. A 60 000 year Greenland stratigraphic ice core chronology. *Clim. Past* **4**, 47–57 (2008).
64. Andersen, K. K. et al. The Greenland Ice Core Chronology 2005, 15–42 ka. Part 1: constructing the time scale. *Quat. Sci. Rev.* **25**, 3246–3257 (2006).
65. Blockley, S. P. E. et al. Tephrochronology and the extended intimate (integration of ice-core, marine and terrestrial records) event stratigraphy 8–128 ka b2k. *Quat. Sci. Rev.* **106**, 88–100 (2014).
66. Arz, H. W., Lamy, F., Ganopolski, A., Nowaczyk, N. & Pätzold, J. Dominant Northern Hemisphere climate control over millennial-scale glacial sea-level variability. *Quat. Sci. Rev.* **26**, 312–321 (2007).
67. Grant, K. M. et al. Rapid coupling between ice volume and polar temperature over the past 150,000 years. *Nature* **491**, 744–747 (2012).
68. De Vivo, B. et al. New constraints on the pyroclastic eruptive history of the Campanian volcanic Plain (Italy). *Miner. Petrol.* **73**, 47–65 (2001).
69. Singer, B. S. et al.  $^{40}\text{Ar}/^{39}\text{Ar}$ , K–Ar and  $^{230}\text{Th}$ – $^{238}\text{U}$  dating of the Laschamp excursion: a radioisotopic tie-point for ice core and climate chronologies. *Earth Planet. Sci. Lett.* **286**, 80–88 (2009).
70. Cullen, V. L., Smith, V. C. & Arz, H. W. The detailed tephrostratigraphy of a core from the south-east Black Sea spanning the last ~60 ka. *J. Quat. Sci.* **29**, 675–690 (2014).
71. Janz, H. & Vennemann, T. W. Isotopic composition (O, C, Sr, and Nd) and trace element ratios (Sr/Ca, Mg/Ca) of Miocene marine and brackish ostracods from North Alpine Foreland deposits (Germany and Austria) as indicators for palaeoclimate. *Palaeogeogr. Palaeoclimatol. Palaeoecol.* **225**, 216–247 (2005).
72. Vasiliev, I., Reichert, G.-J., Davies, G. R., Krijgsman, W. & Stoica, M. Strontium isotope ratios of the Eastern Paratethys during the Mio-Pliocene transition; Implications for interbasinal connectivity. *Earth Planet. Sci. Lett.* **292**, 123–131 (2010).
73. Larsen, E. et al. Late Pleistocene glacial and lake history of northwestern Russia. *Boreas* **35**, 394–424 (2006).

### Acknowledgements

We thank the captain and crew of RV Meteor and the cruise leader Christian Borowski for their support during the M72/5 Black Sea cruise in 2007. Technical/analytical support by Sylvia Pinkerneil and Elmar Reitter is greatly acknowledged. The authors thank two anonymous reviewers for constructive comments that improved the manuscript. This work was funded by the Deutsche Forschungsgemeinschaft (AR 367/9-1, AR 367/9-2, WE 6136/1-1) and by the Gary Comer Science and Education Foundation.

### Author contributions

A.W. and H.W.A. initiated the project, designed the study, and wrote the manuscript. A.W., B.P., I.C.K., and H.W.A. were closely involved in the preparation and isotope analyses of the ostracod samples and during writing of the manuscript.

### Funding

Open Access funding enabled and organized by Projekt DEAL.

### Competing interests

The authors declare no competing interests.

### Additional information

**Supplementary information** The online version contains supplementary material available at <https://doi.org/10.1038/s43247-021-00129-3>.

**Correspondence** and requests for materials should be addressed to A.W. or H.W.A.

**Peer review information** Primary handling editor: Joe Aslin

**Reprints and permission information** is available at <http://www.nature.com/reprints>

**Publisher's note** Springer Nature remains neutral with regard to jurisdictional claims in published maps and institutional affiliations.



**Open Access** This article is licensed under a Creative Commons Attribution 4.0 International License, which permits use, sharing, adaptation, distribution and reproduction in any medium or format, as long as you give appropriate credit to the original author(s) and the source, provide a link to the Creative Commons license, and indicate if changes were made. The images or other third party material in this article are included in the article's Creative Commons license, unless indicated otherwise in a credit line to the material. If material is not included in the article's Creative Commons license and your intended use is not permitted by statutory regulation or exceeds the permitted use, you will need to obtain permission directly from the copyright holder. To view a copy of this license, visit <http://creativecommons.org/licenses/by/4.0/>.

© The Author(s) 2021